Finite element analysis on the wire breaking rule of 1×7IWS steel wire rope

DU Wenzheng, MA Baozhu, XIE Zheng, CAO Dazhi and WU Peng

Xi'an High Technology Research Institutute, China

Abstract. Taking the wire rope of 1×7+IWS structure as the research object, the influences of the number of broken wires on the stress distribution under the same axial load were simulated and analysed, and it also explored the rule of wire breaking of steel wire ropes. Based on the SolidWorks software, the three-dimensional model of the wire rope was established. Importing the model into the ABAQUS, the finite element model of the steel wire rope was established. Firstly 5000 N axial tension was placed on the rope, the stress distribution was simulated and analysed, and the steel wire with the largest stress distribution was found out. Then one steel wire was truncated with the load unchanged, and the finite element simulation was carried out again, and repeated the steps several times. The results show that, with the increase of the number of broken wires, the Von-Mises stress of the wire rope increases sharply, and the stress distribution is concentrated on the rest of the unbroken wires, which brings great challenges to the safety of the wire rope.

1 Introduction

The wire rope is widely used in industrial production and daily life, its performance has important influence on the safety [1]. But the steel wire rope is of space spiral structure which is very complex, therefore the traditional stress analysis can not accurately solve the mechanical properties [2]. At the same time in the process of ascension, due to wear, corrosion, fatigue, impact and other reasons[3], the wire rope is easy to occur the phenomenon of wire breaking .In the fracture failure process of wire ropes, the number of broken wires increases gradually, until the whole wire rope breaks. Therefore, the study of the stress change and wire breaking rules in the process of wire breaking under the same load is very important to prevent the wire rope breaking accidents and improve the level of the use and maintenance of the wire rope. Li Lunyou analysed the reasons of failure of 6*36sw-25.0mm steel wire rope for field bridge through the electron microscope observation[4]. The fatigue damage of the steel wire rope bearing load under different pre tension was studied by fatigue test in Jia Xiaofan[5]. Zhang Lun used scanning electron microscope, energy spectrum instrument for the failure analysis of wire rope for the electric door and window elevator [6].Wei Huaichang elaborated the phenomenon and reason for abnormal wire breaking of the floor type friction wheel winch hoisting rope[7]. Hu Zhihui studied the failure mechanism of double broken line type multilayer winding steel wire rope[8].

In this paper, taking 1×7+IWS steel wire rope as the research object, using the finite element analysis software ABAQUS, simulation analysis was carried out on the wire breaking of the wire rope under axial load of 5000N[9].

2 Finite element model of 1×7+IWS steel wire rope

2.1 Geometry model of the steel wire rope

In this paper, the three-dimensional solid model of 1 * 7 IWS structure round strand wire rope was established by SolidWorks software. The twist moment is 42.3mm, the diameter of the rope core and the side strand wire are both 2.34mm. The steel wire rope structure is shown in Figure 1.

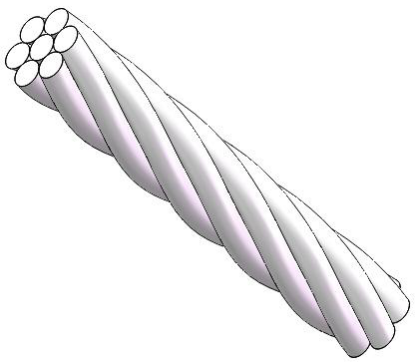

Figure 1. The geometric model of the 1×7+IWS steel wire rope

In order to reduce the amount of calculation, using wire rope cyclic symmetric structure characteristics, 1/6

twist length (7.05mm)of the wire rope was intercepted as the research object, which was imported directly into ABAQUS software through the SolidWorks and ABAQUS plug-in interface. According to the result of each simulation, the steel wire which has the maximum stress is cut off in turn, to create a new assembly, and the simulation analysis is carried out again.

2.2 Material properties

The material of steel wire rope core and side wires is a high-quality carbon steel, for isotropic materials, and the specific parameters are shown in Table 1 [10].

Table 1. The material properties of the steel wire rope

Density ρ (kg/m^3)	Poisson's ratio γ	Elastic modulus$E$(Gpa)	Yield strength σ_s (Mpa)	Limitssing intensity σ_b (Mpa)
7800	0.3	200	1670	1803.5

2.3 Element mesh division

The rope core and side strands wires all used C3D8I unit (8-node linear hexahedral elements, incompatible mode). By means of the method of the neutral axis, the wire rope was meshed [11]. In the process of finite element simulation, in order to ensure the convergence results, the mesh need to be gradually refined to determine appropriate grid density according to the calculation results of different grid density. Through the calculation and test, the finite element model of steel wire rope was determined, as shown in Figure 2. The total cell number of the finite element model of the whole wire rope is 139264, and the total number of the nodes is 155382.

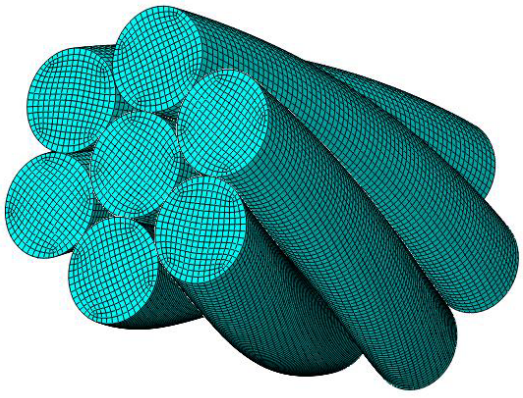

Figure 2. The finite element mesh of the 1×7+IWS wire rope

2.4 Contact attributes

As shown in Figure 3, the master-slave contact algorithm is applied to transfer load between the two contacts. According to the principle that slave surfaces can be penetrated, but main surfaces can not be penetrated [12], each wire can be either the master surface or slave surface to establish contact pairs between adjacent wires. Also finite sliding mode was selected between two contact surfaces. The friction coefficient between the steel wires was defined as 0.1 [13], and the friction type is penalty function.

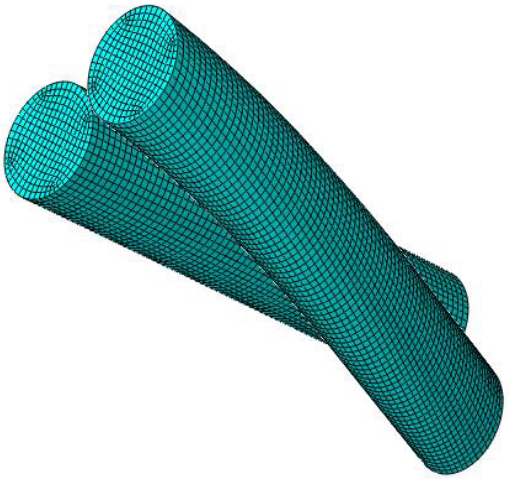

(a) The contact pairs of the wire and straight strand rope core

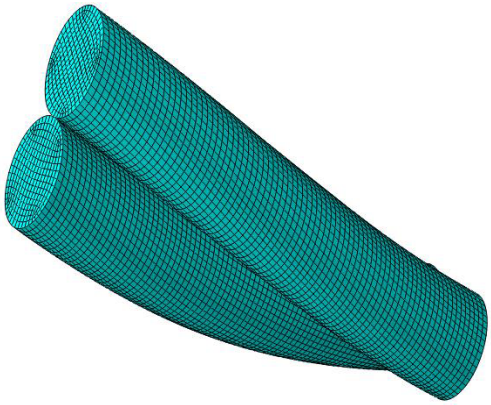

(b) The contact pairs of the wires

Figure 3. The contact model of the wire rope

2.5 Boundary conditions and loading methods

Reference points are established respectively in the axis of the rope core and they are located at the center of the front surface and back surface of the wire rope to couple all the nodes of the corresponding cross-section. Each reference point has six degrees of freedom, namely, three translational degrees of freedom and three rotational degrees of freedom. In finite element analysis of wire rope, the model of coupling movement establishes a relationship of motion constraints between each node and reference point in the bound area. And it makes the reference point and the nodes of the bound area achieve the same displacement [14]. In the finite element analysis, all the degrees of freedom of one point were constrained and 5000N axial tensile load was placed on the other reference point.

3 Finite element simulation

3.1The first simulation (0 broken wires)

The 5000N axial tension was applied at the reference point 2, and the finite element simulation was carried out, and the analysis results are shown in Figure 4 and Figure 5.

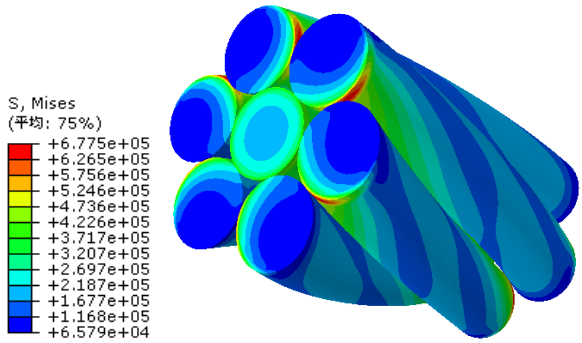

Figure 4. The Von-Mises stress distribution of the wire rope

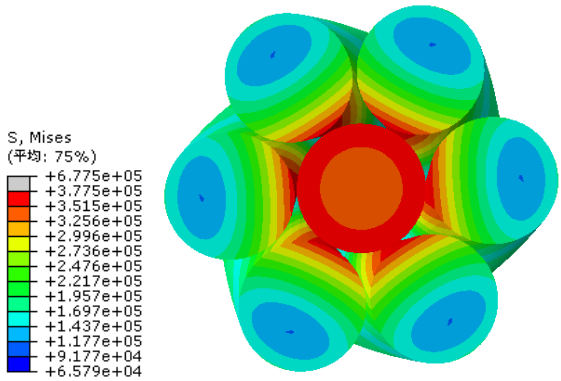

Figure 5. The stress distribution at cross section of the rope

On the whole wire rope, due to the constraints of the coupling movement on both ends of the wire rope, the stress on both ends is large while the stress in the central area is small. On the end face of the wire rope, the stress distributes radially around the rope core, the stress on the contact of wires is larger than other area. On the face of the rope core, the stress distributes like concentric circle. The central stress is the minimum while the outer stress is the maximum. Besides, the six side wires share the same stress distribution on the surface, which is consistent with the symmetry of the geometry model. On the side of the wire rope, the stress presents a helix staggered distribution along the surface of the spiral steel wire.

In order to reduce the influence of coupling constraint on the results, the intermediate section of the wire rope is taken as the research object, and the von-mises stress distribution is observed, as shown in Figure 5. For the whole cross section, the von-mises stress distribution around the center of the wire rope is symmetrical, and the stress of the rope core is the largest of the cross section. The stress on the rope core presents concentric circular distribution, and the stress on the contact area between the core and the side strand wire is 373.470MPa, which is the largest of the whole wire rope. For each side wire, the stress distribution is layered. From the center to the outside, the stress decreases gradually.

3.2 The second simulation (1 broken wires)

It is concluded from the first simulation that the stress on the rope core is the largest, and the the rope core is easy to produce fatigue fracture in the process of using. Assuming that the rope core is broken, the rope core is cut off in the three-dimensional model, and the finite element simulation results under the same 5000N axial load are shown in Figure 6 and 7.

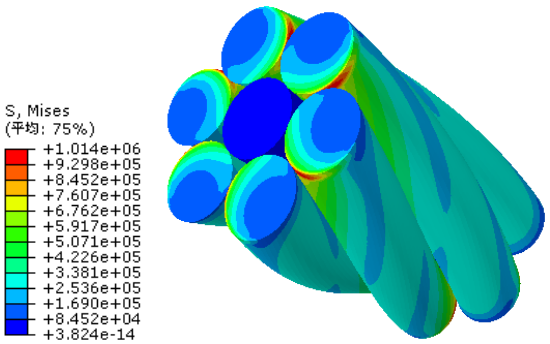

Figure 6. The Von-Mises stress distribution of the wire rope

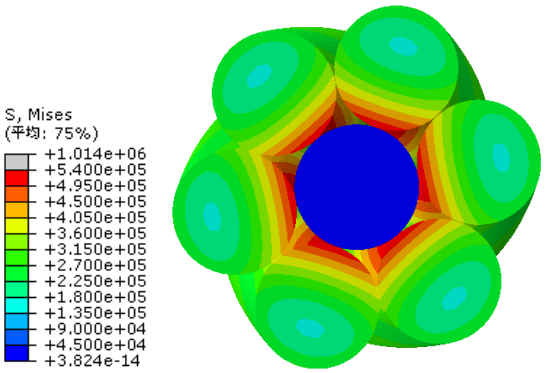

Figure 7. The stress distribution at cross section of the rope

Because the rope core is broken and it can not bear the load, the stress of the whole rope core is close to 0. The rest six side strand steel wires bear the axial tensile strength of 5000n, therefore the stress is increased significantly. On the middle cross section of the steel wire rope, the stress of the contact area between the side strand and the rope core is the largest which is 528.695MPa.

3.3 The third simulation (2 broken wiress)

It is concluded from the second simulation that the stress on the side strand is the largest of the rope, therefore it is easy to break during the working process. Assuming that a strand of wire rope is fractured, it is cut off in the three-dimensional model of the wire rope as well. Under the same 5000N axial load, the finite element simulation results are shown in Figure 8 and 9.

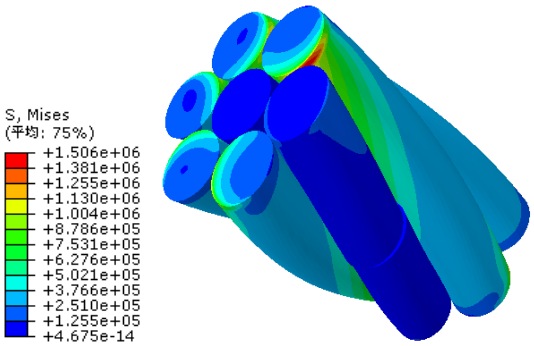

Figure.8 The Von-Mises stress distribution of the steel wire rope

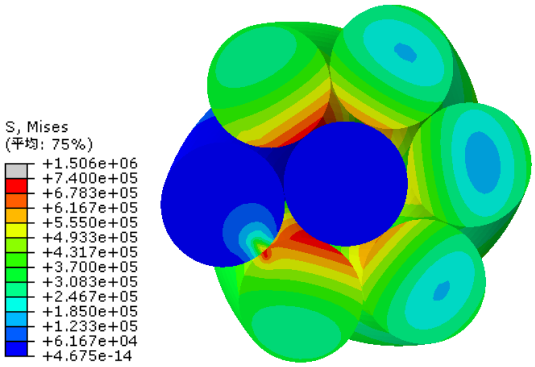

Figure.9 The stress distribution at cross section of the wire rope

The rope core and a side strand wire are broken, which can not bear the load, only play a supporting role, therefore its stress is close to 0.The axial tension of 5000N is fully suffered by 5 side strand steel wires and the stress distribution on each side strand is different, and the upper limit of the stress is increased significantly. From Figure 9, we can find that the maximum stress is distributed on the two side strand wires which are adjacent to the fractured side strand and the maximum stress is 719. 964MPa.

3.4 The fourth simulation (3 broken wires)

It is concluded that the maximum stress is distributed on the two side strand wires which are adjacent to the fracture side strand wire from the third simulation. Assuming that one side strand wire breaks in the course of work, it is cut off in the three-dimensional model of the wire rope, and the finite element simulation results under the same 5000N axial load are shown in figure 10 and 11.

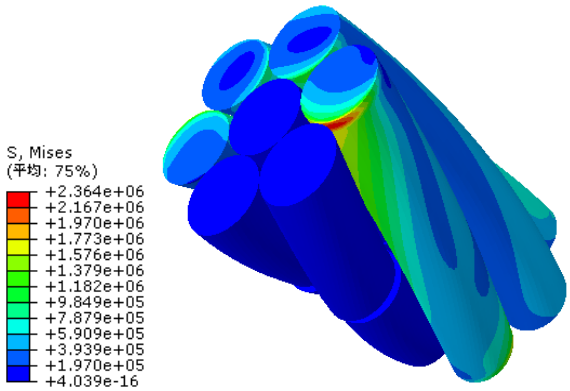

Figure 10. The Von-Mises stress distribution of the wire rope

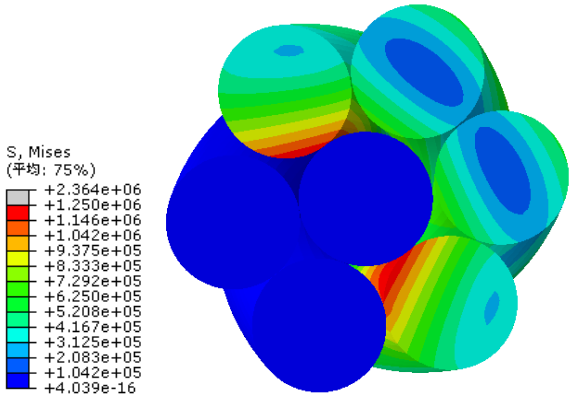

Figure 11. The stress distribution at cross section of the rope

The rope core and the two side strand wires are all broken, which can not bear the load, only play a supporting role, therefore its stress is close to 0. The axial tension of 5000N is fully suffered by 4 side strand steel wires, and the stress on the side strand wire increases significantly. The maximum stress is distributed on the two side strand wires which are adjacent to the fracture side strand wire, which is 1207.99 MPa. Compared with the third simulation results, the stress is greatly increased.

3.5 The relationship between stress,deformation and the number of broken wires

The four simulation results show that the Von-Mises stress is increasing with the increase of the number of broken wires, under the same load. The maximum stress σ_{max} and the maximum axial deformation U_{max} of the four simulations are distilled, as Table 2 shows, and the relation curves are shown in Figure 12 and 13.

Table 2. The corresponding value of σ_{max} $U_{max}$and μ

Number of broken wires n	0	1	2	3
Von-mises σ_{max}/MPa	373.470	528.695	719.964	1207.99
Axial deformation U_{max}/mm	0.0179	0.02654	0.04512	0.1078

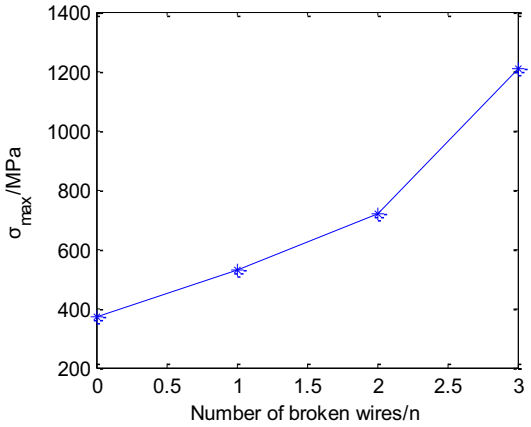

Figure 12.The relation curve of σ_{max} and n

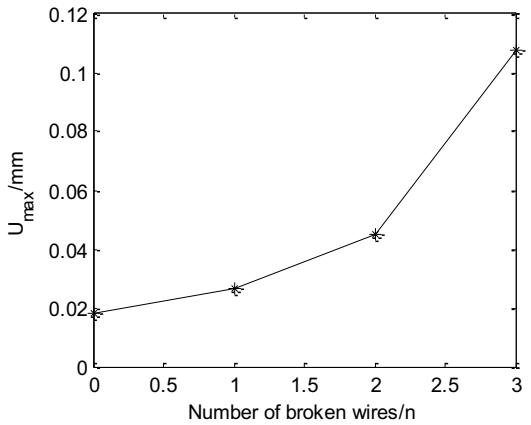

Figure 13.The relation curve of U_{max} and n

As Figure 12 and 13 show , under the same load, the maximum von Mises σ_{max} and axial deformation U_{max} are increased with the increase of the number of broken wires n, and the increasing speed is faster and faster. Therefore, with the increase of the number of broken wires n, anti load capacity of the wire rope decreases sharply, and the wire rope is more easy to be broken.

4 Conclusions

This paper analysed the influence of the number of broken wires on the stress distribution and the axial deformation of 1×7+IWS steel wire rope under the same axial load and explored the rule of the broken wires. The conclusions can be drawn as follows:

1). With the increase of the number of broken wires n, the von-mises stress of the steel wire rope increases rapidly under the same load. The greater the stress, the more serious the wear of the wire rope, and the shorter the fatigue life.;

2). With the increase of the number of broken wires n, the axial deformation is also increasing rapidly under the same load, which bring adverse effects on the steel wire rope;

3). The broken wires almost no longer bear the axial load, only play a supporting role, and the steel wire adjacent to the broken wire will bear larger load. It is easy to produce stress concentration, which accelerates the damage process.

References

[1] Li Zhanfang, Xiao Xingming, Liu Zhengquan, et al. Study on dynamics of mine hoisting rope [J]. Coal mine safety, 10:11-14, (2007)
[2] Hruska F.H.Radial forces in wire ropes[J].Wire Produets, 2(7): 459-463, (1952).
[3] Lv Xiaohui, Chen Zhiping, Wang Songgen, et al. Study on the failure mechanism of steel wire rope [J]. Metal products, 39 (5): 1-5, (2013).
[4] Li Lun you, Zhang Xiaoyan, Zhang Qi. Failure analysis of broken wire of 6*36sw-25.0 mm steel wire rope used by a bridge [J]. Guizhou industry university journal, 35 (1): 43-45, (2006).
[5] Jia Xiaofan, Zhang Dekun. Research on bending fatigue damage of bearing steel wire under different pre tension [J]. Journal of mechanical engineering, 47 (24): 31-37, (2011).
[6] Zhang Lun, Liu Hongfang, Sun Jie. Fatigue fracture analysis of steel wire rope for electric door and window elevator [J]. Metal products, 39 (1): 56-59, (2013).
[7] Wei Huaichang. Analysis and solution of the broken wire of winch lifting wire rope [J]. Coal mine machinery, 28 (11): 176-177, (2007).
[8] Hu Zhihui, Hu Yong, Hu Jiquan, et al. Study on the failure mechanism of the double broken line multilayer winding steel wire rope [J]. China Mechanical Engineering, 24 (23): 3195-3199, (2013).
[9] Zhang Min, Kou Ziming, Li Ting. Torque analysis of steel wire rope based onABAQUS [J].Coal mine safety, ,47 (2): 113-115, (2016).
[10] Zhang Jin, Chen Xiangyang, Tang Wenting, et al. Finite element analysis of.1 * 7 IWS structural steel wire rope [J]. Journal of Anhui University of Science and Technology, 34 (3):83-86, (2014).
[11] Zhang Jianwei. Abaqus 6.12 finite element analysis from entry to the master [M]. Beijing: Mechanical Industry Press, 87-132.
[12] Shi Yiping, Zhou Yurong. Abaqus finite element analysis of detailed examples [M]. Beijing: Mechanical Industry Press, 2015:136-140, (2015).
[13] Wang Dagang. Fretting and fretting fatigue life prediction of steel wire rope [D]. Xuzhou: China University of Mining and Technology, (2012)
[14] Zhu Wenmin, Zheng Gang, Liu Zhicai, et al. Analysis of stress and fatigue of steel wire rope based on Ansys Workbench [J]. Lifting and transportation machinery, (2): 34-38, (2016)